Capitalizing on the High Mass Accuracy of Electrospray Ionization Fourier Transform Mass Spectrometry for Synthetic Polymer Characterization: A Detailed Investigation of Poly(dimethylsiloxane)

E. Peter Maziarz III, Gary A. Baker, and Troy D. Wood*

Department of Chemistry, Natural Sciences Complex, State University of New York at Buffalo, Buffalo, New York 14260-3000

Received December 3, 1998; Revised Manuscript Received April 9, 1999

ABSTRACT: We report on the use of electrospray ionization Fourier transform mass spectrometry (ESI−FTMS) toward the detailed analysis of a commercial poly(dimethylsiloxane) (PDMS) polymer sample. The high mass resolving power (accurate mass measurement), typical in FTMS analysis, allowed structural identification of all observed oligomeric manifolds. Such manifolds represent intact PDMS oligomers, various PDMS fragment ions, and polymer impurities. Further, we demonstrate the utility of nozzle−skimmer dissociation (NSD) not only in end-group analysis but also in the determination of whether an oligomeric distribution is the result of an energetic fragmentation route or is present as an impurity. Specifically, the relative ion intensities of the distribution of interest were examined before and after induced NSD conditions. Until recently, such ESI−FTMS techniques have been primarily used for the analysis of biopolymers. Taken in whole, these data demonstrate the utility of these methods toward the characterization of hydrophobic synthetic polymeric samples, structurally and mechanistically, with potential toward the investigation of real world polymeric samples.

Introduction

By merit of its inherent high sensitivity, broad dynamic range, specificity, selectivity, and information-rich nature combined with broad applicability, mass spectrometry (MS) has become an indispensable analytical tool for the structural characterization of organic and inorganic polymeric materials. No longer in the formative stages, MS capabilities have, over the last 3 decades, evolved to such a degree that a repertoire of MS techniques, powerful deconvolution and data reduction algorithms, and interpretation methods exist to provide, with speed and precision, detailed information about oligomer and polymer distributions and interactions, fingerprint identification patterns, repeat unit and end group sequences, branching, cross-linking or other side-chain substitution, evidence for copolymers, additives, impurities or modifications, and molecular weight distributions.[1−11] Molecular weight and molecular weight distribution are key, fundamental properties of a polymeric material because the combined influence of the constituents relates to properties such as tensile strength, brittleness, osmotic pressure, melt viscosity, refractive index, solubility, adhesion, and abrasive and chemical resistance.[12,13] While most molecular weight characterization methodologies (nephelometry, binding affinity to a stationary phase, or techniques based on thermodynamic or colligative properties) rely on correlating indirect properties to relative molecular weight, mass spectrometry makes possible the direct determination of the molecular masses of individual oligomers, without reference to known, preferably monodisperse, costly standards. By steric and polar interactions, the pendant groups tethered to a polymer skeleton may also exert a profound influence on polymer solubility, susceptibility to cleavage, glass phase transition temperature (T_g), crystallinity, and general surface properties. While polymer structural investigations may be advanced by generating fragments characteristic of the backbone or such pendant groups, this often presents a problem because polymers having similar structures generally follow similar fragmentation mechanisms resulting in nearly identical spectra at low *m*/*z*. Distinguishing between similar polymers thus requires that different molecules be ionized and analyzed with similar efficiency and with minimal dissociation because larger mass fragments provide unambiguous structural information. Fortunately, the challenging problems associated with polymeric ionization have been well met by various innovative soft ionization techniques such as field desorption (FD),[14,15] ^{252}Cf plasma desorption (PD),[16,17] fast atom bombardment (FAB),[18,19] desorption chemical ionization (DCI),[20] secondary-ion mass spectrometry (SIMS),[21−23] matrix-assisted laser desorption/ionization (MALD/I),[24−27] direct laser desorption (LD),[28] and electrospray ionization (ESI).[29−38]

Although, like FAB and MALD/I, progress in ESI is commonly measured relative to its impact on the studies of easily ionizable, hydrophilic biomolecules, significant contributions in this area have also been made in the analysis of synthetic polymers. ESI is an attractive ionization choice because of several intrinsic advantages including minimal fragmentation, high ionization efficiency, and the multiplicity of charges (*z*) placed on each ion, yielding a high mass (*m*) range even for limited *m*/*z* range analyzers. ESI−MS, in principle, facilitates the detection of oligomeric or polymer species (with little or no fragmentation, unless so promoted or controlled by ancillary means) to give accurate macromolecular masses, allowing the determination of polymer structure, including that of end groups, in addition to yielding number- and weight-average-derived molecular masses. Further, ESI does not require selection of a matrix, and it is particularly well suited for use with Fourier transform mass spectrometry (FTMS), well-known for

* To whom correspondence should be addressed. Phone: 716-645-6800 ext. 2176. Fax: 716-645-6963. E-mail: twood@acsu.buffalo.edu (E-mail).

10.1021/ma981877+ CCC: $18.00
Published on Web 05/27/1999

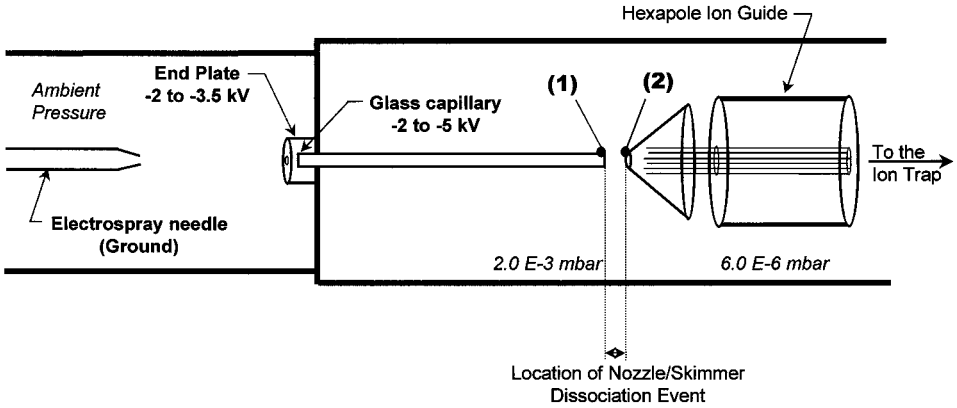

Figure 1. Schematic diagram of the external ESI source used in this experiment: (1) applied capillary potential; (2) applied skimmer potential.

its high mass range and ultrahigh mass resolving power (RP) as well as the its facility for multistage tandem mass spectrometry (MS^n). Compared with the 10^2-10^3 RP typical of quadrupole and time-of-flight mass spectrometers, FTMS routinely offers RP of $\sim 10^5$ (high enough to resolve $^{12}C/^{13}C$ isotopic peaks) even above 25 kDa.[39−42] Such a RP is of paramount importance when distributions stemming from the range of oligomeric species present in a polydisperse sample overlap with those arising from the multiple charging during the ESI process to produce complex and highly convoluted spectra. Further, by meeting the severe mass resolution demands, hyphenation of ESI−MS to condensed-phase separation techniques in often unnecessary.

Synthetic polymers present a particularly challenging scenario because their solubilities often limit their use to ESI unfriendly solvents. Furthermore, the chemical structure may preclude in situ ion formation by prohibiting the ESI mechanism. Despite impediments associated with electroneutrality, synthetic polymer systems studied by ESI−MS to date include poly(ethylene glycol),[33,35,38] poly(amidoamine) starburst dendrimers,[43] polyester resins,[38,44] octylphenoxypoly(ethoxy)ethanol,[45] poly(methyl methacrylate),[36,46] caprolactones,[47] poly(tetrahydrofuran),[36] polystyrene,[36,48] and polysulfides.[49] To our knowledge, this is the first report detailing the use of ESI−MS toward poly(dimethylsiloxane) (PDMS) analysis.

Here a commercial external electrospray ionization Fourier transform mass spectrometer (ESI−FTMS) was used to perform a detailed study of a PDMS polymer with (aminopropyl)dimethylsiloxy (APS) termini. We report less than 10 ppm error between experimental and theoretical mass values for all distributions observed in the mass spectrum. From this exact mass data we obtained the elemental composition for each distribution and proposed structures for each. Furthermore, nozzle−skimmer dissociation was used to determine end group chemistry and to gain insight into two specific distributions known from their mass not to represent intact APS−PDMS. Where applicable, proposed fragmentation mechanisms for the formation of these distributions are given.

Experimental Section

ESI−FTMS Instrumentation. All experiments were performed on a Bruker (Billerica, MA) BioApex 30es Fourier transform mass spectrometer. The instrument design and a description of the 3.0 T magnet and pumping system used have been reported elsewhere.[50] This instrument is equipped with an Analytica of Branford (Branford, CT) ESI source that contains a radio frequency (rf) only Iris hexapole ion guide that can be used to externally accumulate ions. A Cole-Palmer (Vernon Hills, IL) series 74900 infusion pump was used to inject analyte samples continuously into the ESI source at a rate of 60 μL h^{-1}. Nitrogen countercurrent drying gas (250 °C) at a flow rate of 10−15 L min^{-1} was used to desolvate droplets produced by the ESI source. A potential between −3.2 and −3.8 kV (relative to the grounded needle) was applied to the metal-capped glass capillary. Ions were electrostatically injected into the Infinity cell[51] (2.0 V trapping potential) using the patented Sidekick method.[52] Frequency-sweep excitation from m/z 400 to 2500 was applied at an amplitude of ∼44−63 V_{pp}. Detection was in direct mode (500 kHz Nyquist bandwidth) from time domain data sets of 128K (25 scans/experiment). The data sets were apodized with a Gaussian function, Fourier transformed, and displayed in magnitude mode. The instrument was calibrated from ion products generated by a 30 μM, 2 kDa standard poly(ehtylene glycol) sample.

Sample Preparation. The following materials were used in these experiments: PDMS 2500 with (aminopropyl)dimethylsiloxy (APS) termini (Sigma Chemical Co.), methanol (HPLC grade, Mallinckrodt), 2-propanol (Fisher Scientific), and sodium hydroxide pellets (99.99% semiconductor grade, Aldrich Chemical Co., Inc.). All PDMS samples were prepared as 30 μM solutions in a solvent system composed of methanol/2-propanol/acetic acid (49:49:2, v/v/v). All reagents were used as received and without further purification.

Nozzle-Skimmer Dissociation. Ions formed by the ESI process begin at atmospheric pressure whereupon they experience a negative pressure gradient until they reach their final destination within the mass analyzer (i.e., ion trap, quadrupole mass filter) with typical pressures in the $10^{-7}-10^{-10}$ mbar regime. Transfer of ions through such a pressure gradient is generally achieved via ion optics such as electrostatic lenses. Figure 1 illustrates a simplified diagram of the ESI source used here. Within our ESI source, the accumulation region (containing five loci of applied dc potential surrounding six rf-only rods) is the first stage at which ions are effectively focused through the differential pumping regions. For this portion of the work, we focus on the region of space between the capillary and skimmer electrodes where ions experience a supersonic expansion event and subsequent collisions with background gas. The potentials applied at the capillary and skimmer electrodes serve to accelerate and focus the ions through this intermediate region. Increasing the acceleration of ions through this region, by modulating the voltage bias between the capillary and skimmer electrodes, can result in fragmentation of molecular ions by enhancing the effectiveness of collisions with background gas. This class of collision-induced dissociation (CID) is commonly referred to as "nozzle−skimmer dissociation" (NSD) or "source−skimmer CID" and has been used to obtain partial sequence information about proteins and structural detail for analyte ions including the determination

Table 1. Proposed Molecular Identities of All Oligomeric Distributions Observed in the Analysis of APS−PDMS Polymer

Suspected Oligomer	Dist.	End Group and charge reagent masses (Da)	Deg. of Poly. (n)	Theoretical Mass	Experimental Mass	Error (ppm)
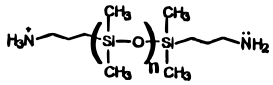	Δ	58.0651 116.0890 1.0073	13	1137.4067	1137.4121	4.7
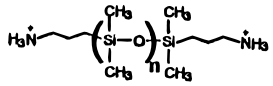	o	58.0651 116.0890 1.0073 1.0073	29	2322.7152	2322.7144	0.3
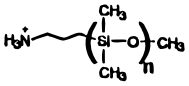	♦	58.0651 15.0229 1.0073	14	1110.3595	1110.3599	0.4
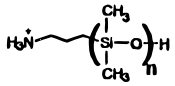	□	58.0651 1.0073 1.0073	15	1170.3626	1170.3588	3.2
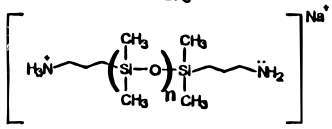	●	58.0651 116.0890 1.0073 22.9898	29	2344.6971	2344.7194	9.5
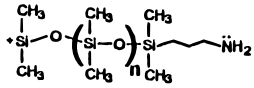	*	74.0182 116.0890	13	1152.3520	1152.3610	7.8

of polymer end groups. The theoretical considerations for this phenomenon have recently been detailed by Hunt et al.[38] It should be noted that the numerical values of the applied potentials at the capillary and skimmer electrodes are semi-empirical as they are both molecule and source dependent. Rather, it is the potential difference between the capillary and skimmer electrodes that give rise to NSD conditions. Comparatively, the larger potential difference results in a higher collisional energy between analyte and background gas. For the NSD study all spectra were collected under the same experimental conditions while the potential difference of the capillary and skimmer electrodes were increased, and the actual values for these potentials are given with the data where appropriate.

Data Analysis. The charge state (z) of each oligomer was determined from the m/z difference of $^{12}C/^{13}C$ isotope peaks, and therefore the mass ($m/z \times z$) of each peak in the spectrum could be obtained. The abundance (a_i) of an oligomer was obtained by summing the abundances of all peaks in the isotope-cluster distribution. The mass of such an oligomer (m_i) was determined from the monoisotopic peak in the isotope-cluster distribution. The degree of polymerization (n) was obtained by subtracting the monoisotopic masses of the end groups and charge agents from m_i and dividing by the monoisotopic mass of the siloxane repeat unit (74.0182 Da). A composite molecular weight distribution was obtained from the summation of ion intensities with corresponding (n) values throughout all charge states of intact PDMS polymer (○ and Δ). From this distribution M_w and M_n were calculated.

The relative ion intensity data presented herein represents the signal of the monoisotopic peaks from each isotope cluster relative to the same nominal size oligomer before and after nozzle−skimmer dissociation. Because this comparison is relative to the same mass (for each nominal oligomer), any change in ion intensity is due to an experimental condition (NSD) and not due to statistical variation of isotope abundance. This method of comparison enables a more accurate description for the (□) distribution where spectral overlap with the (●) distribution is significant at the third through sixth isotopic peaks but is obsolete at the first (mono) isotopic peak.

Results and Discussion

Spectra of (Aminopropyl)-Terminated PDMS. The high mass resolving power capability of FTMS leads to accurate mass measurements, enabling the elucidation of polymer features such as repeat unit and terminal mass. It should be noted that such mass data do not provide *direct* structural information of a polymer. However, from these data one can obtain the elemental composition of the polymer that can be used to propose a structure. Table 1 summarizes proposed molecular structures for the mass spectral PDMS distributions observed in this paper. These molecular structures were determined by comparing experimental masses to theoretical masses generated from assumed molecular structures. Positive identification of these oligomers is corroborated by the low parts per million (ppm) error (less than 10 ppm in all cases). Figure 2 illustrates an ESI-MS of 30 μM, nominally 2500 Da, APS-terminated PDMS. Preformation of a charged analogue of this species in solution is readily obtained by protonation of basic free amines residing on the terminal ends of the polymer. The Figure 2 inset provides an expanded view of the distributions observed in this mass spectrum. Two distinct, intense distributions are apparent. The first, denoted by (Δ), corresponds to peaks belonging to a +1 charge state (CS)

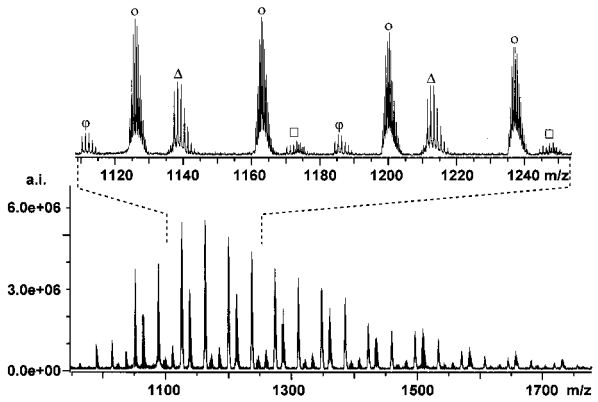

Figure 2. ESI−FTMS of 2500 Da APS−PDMS polymer, sum of 25 scans.

distribution of intact APS−PDMS oligomers. The repeat unit mass is calculated from the *m*/*z* difference of two adjacent oligomeric peaks within a given CS manifold. For this and all other distributions in this spectrum, the nominal repeat unit mass is 74 Da, corresponding to the mass of a dimethylsiloxane subunit ($Si(CH_3)_2O$). The second series, denoted by (*o*), corresponds to the peaks that belong to the +2 CS distribution of intact APS−PDMS oligomers. Molecular weights and their distributions for any given technical polymer are evaluated according to the number-average molecular weight (M_n), the weight-average molecular weight (M_w), and polydispersity (D). M_n is a simple arithmetic mean defined in eq 1 where m_i is the mass and n_i is the

$$M_n = \frac{\sum m_i n_i}{\sum n_i} \quad (1)$$

intensity of the *i*th oligomer in a distribution. M_w is calculated according to eq 2. Polydispersity, D, is

$$M_w = \frac{\sum m_i^2 n_i}{\sum m_i n_i} \quad (2)$$

calculated from M_n and M_w as shown in eq 3 and reflects

$$D = M_w/M_n \quad (3)$$

the overall breadth of the oligomer distribution. Deconvolution of these two CS distributions for APS−PDMS allows calculation of M_w, M_n, and D, which yield values of 2360 Da, 2323 Da, and 1.016, respectively. To construct a true polymer molecular weight distribution, it is a prerequisite for every ion within such a distribution to be detected with equal probability. Unfortunately, confinement of ions within the trap is largely kinetic energy dependent. Hence, mass discrimination effects can occur which result in misrepresented molecular weight distributions for polydisperse ($D > 1.2$) polymers.[27,35,53] For this reason, GPC fractions ($D \sim 1.0$) are oftentimes analyzed off- or on-line to the mass spectrometer so that a true molecular weight distribution can be obtained.[54,55]

In addition to the two intense distributions of intact APS−PDMS, there are also two minor distributions indicated by □ and ϕ. Hercules and co-workers have studied the fragmentation mechanisms of polysiloxanes with different pendant functionalities and end groups by TOF−SIMS.[22,56−58] Among these studies, these researchers reported on general PDMS fragmentation mechanisms which help account for the formation of the □ and ϕ distributions.

The □ distribution can be rationalized by a hydrogen-transfer mechanism similar to the one proposed by Dong et al.[56,57] Such a mechanism is illustrated in Scheme 1 using APS−PDMS as an example. By this mechanism, intact singly charged APS−PDMS oligomer(s) (△) undergo hydrogen transfer from a terminal methyl group to an adjacent oxygen atom, resulting in a distribution of PDMS oligomers (□) that are terminated by a propylamine on one end and a hydrogen atom on the other. Thus, the *m*/*z* 115 shift (from △ → □) reveals useful quasi-molecular information about one of the polymer end groups. Such fragment data are useful in the determination and verification of the chemical makeup of a polymer or polymer blend. It should be

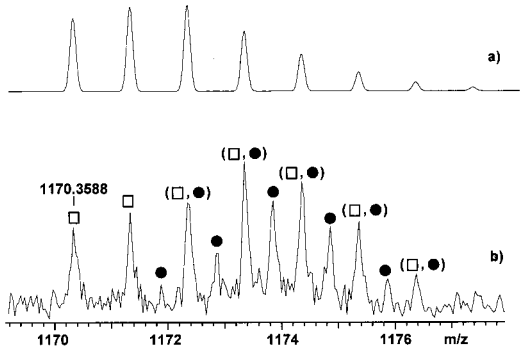

Figure 3. (a) Theoretical and (b) experimental isotopic distribution for $Si_{15}C_{33}N_1H_{100}O_{15}$ in the □ distribution.

Scheme 1. Proposed Hydrogen Exchange (Energetic) Fragmentation Mechanism for APS−PDMS Polymer

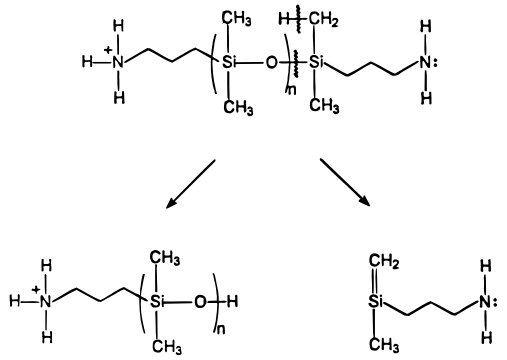

noted that here one of the propylamine end groups is contained within the *m*/*z* 115 fragment. Further, this mechanism indicates that the charge is localized on the end group opposite to the methyl terminus involved in hydrogen transfer. Had this mechanism initiated at the end group possessing the charge, a neutral, ergo undetectable, APS−PDMS fragment would have resulted. An experimental isotopic distribution for an oligomer ($Si_{15}C_{33}N_1H_{100}O_{15}$) in the (□) distribution is presented in Figure 3b. Careful examination indicates that there is an overlapping +2 CS distribution, denoted by ●, which can be attributed to an intact monoprotonated and monosodiated APS−PDMS oligomer. Figure 3a illustrates a theoretical isotopic distribution pattern for $Si_{15}C_{33}N_1H_{100}O_{15}$ that would have resulted from Scheme 1. The small differences in isotopic peak intensities for the theoretical and experimental isotope patterns can be attributed, in part, to the overlapping isotopic peaks from the ● distribution. Peaks that are affected by this overlap are denoted □ and ● in Figure 3b. In a more quantitative fashion, the experimental monoisotopic peak at *m*/*z* 1170 in Figure 3a was compared to the theoretical monoisotopic mass of the $Si_{15}C_{33}N_1H_{100}O_{15}$ oligomer. The nominal (3.2 ppm) deviation between theory and experiment lends overwhelming evidence in support of $Si_{15}C_{33}N_1H_{100}O_{15}$ as the fragment's proper identity.

The origin of the ϕ distribution proved to be more challenging to elucidate. An experimental isotopic distribution for an oligomer of the ϕ distribution is provided in Figure 4a. In an attempt to identify the molecular composition of this oligomer, a database was assembled containing possible PDMS oligomers possessing different end groups. The monoisotopic end group and charging agent masses of each permutation were then subtracted from the experimental monoisotopic peak (*m*/*z* 1110.3599) of Figure 4b. This value was then divided

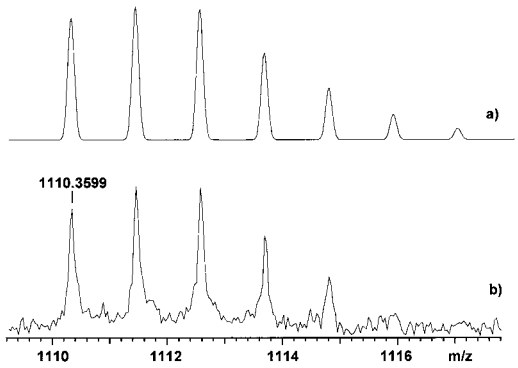

Figure 4. (a) Theoretical and (b) experimental isotopic distribution for $Si_{14}C_{32}N_1H_{96}O_{14}$ in the ϕ distribution.

Table 2. Proposed Molecular Identities for the ϕ Oligomeric Distribution with the Suspected Identity Highlighted

Suspected Oligomer	End Group Masses (Da)	Charge Agent	Degree of Poly. (n)	Theoretical Mass of Oligomer (Da)	Error (ppm) from Experimental Mass (1110.3599 Da)
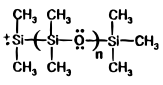	73.0468 74.0182	•+	13	1109.3093	1017.8
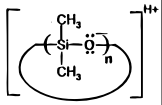	——	H+ (1.0073 Da)	15	1111.2885	892.0
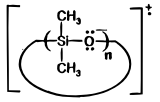	——	•+	15	1110.2807	80.5
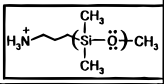	58.0651 15.0229	H+ (1.0073 Da)	14	1110.3595	0.4

by the monoisotopic mass of the dimethylsiloxane repeat unit to determine the degree of polymerization (n). An empirical formula for the oligomer in question was then constructed for recovered integer values of n, the composition of the end groups, and the charging agent. The theoretical monoisotopic mass of this suspect oligomer was then compared with the experimental monoisotopic mass in Figure 4b. Several of these results are summarized in Table 2. The possibility of a cyclic oligomer was also considered, and originally favored, in light of the fact that randomly coiled PDMS chains can undergo intramolecular interaction to result in the formation of both a cyclic and a linear fragment.[56] However, the large error (ca. 80 ppm) associated with this suspected oligomer discounts it as a possible identity for the ϕ distribution. However, we can, with some confidence, assign the identity of said oligomer to the form highlighted in Table 2 by merit of the low error (0.4 ppm) in comparison to the experimentally determined mass. The theoretical isotopic distribution for the $Si_{14}C_{32}N_1H_{96}O_{14}$ oligomer is displayed in Figure 4a. There is good correlation between the experimental and theoretical isotopic distributions.

The existence of the ϕ oligomeric distribution could result from two disparate mechanistic pathways. One possibility is fragmentation of an APS−PDMS oligomer that results in a methyl transfer, as shown in Scheme 2. This mechanism is analogous to the hydrogen-transfer mechanism mentioned earlier. The net enthalpy changes (ΔH) involved in the formation of fragment PDMS ions as depicted by Schemes 1 and 2 can be estimated by appropriate substitution of the bond

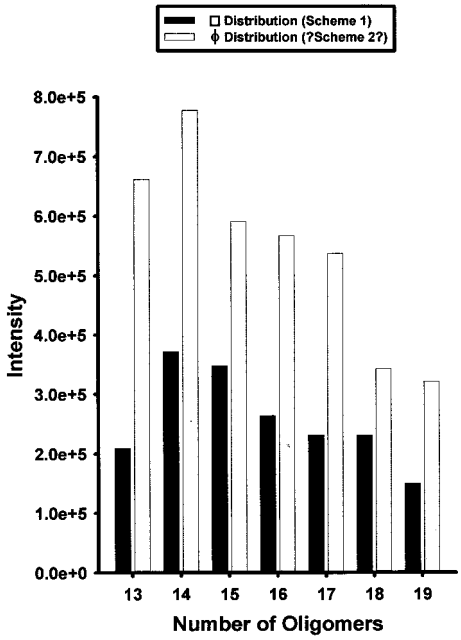

Figure 5. Plot of relative ion intensities for oligomers in the □ and ϕ distributions. Data obtained from Figure 1.

Scheme 2. Possible Methyl Exchange (Energetic) Fragmentation Mechanism for APS−PDMS Polymer

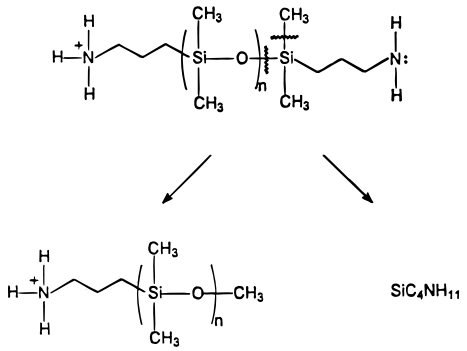

energies (BE) required to form the fragment in question from the precursor ion:

$$\Delta H = \sum \mathrm{BE_B} - \sum \mathrm{BE_F} \qquad (4)$$

where the subscripts B and F refer to bonds broken in the precursor and formed in the product, respectively. Our intention here is not to imply that we are measuring enthalpy per se, which requires that pressure remain constant. Rather, we wish to simply make a zeroth-order approximation and compare the energy required for two identical molecules, analyzed under the same experimental conditions, to follow different fragmentation routes. We estimated, from literature bond energy data,[59] that formation of the fragment oligomer in Scheme 2 from intact APS−PDMS requires approximately 893 kJ/mol of energy. In comparison, an energy of only 710 kJ/mol is required for formation of the analogous fragment ion by Scheme 1. Assuming that the □ and ϕ distributions arise from energetic fragmentation mechanisms alone, one would thus expect the hydrogen-transfer mechanism (Scheme 1) to dominate because it is less demanding energetically. This is, however, contrary to what is observed in Figure 5, where the relative ion intensities of the ϕ oligomers (Scheme 2) are larger than those of the corresponding

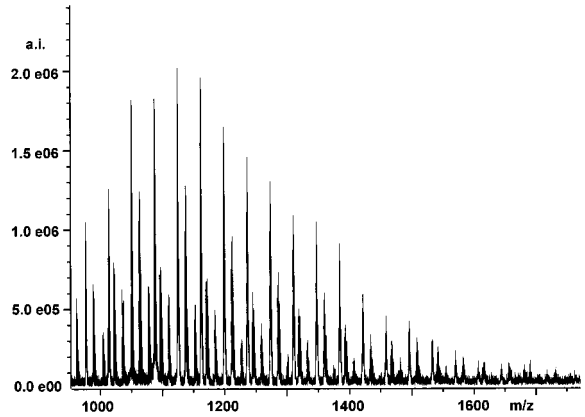

Figure 6. ESI−FTMS of 2500 Da APS−PDMS polymer after induced nozzle−skimmer dissociation (NSD), sum of 25 scans.

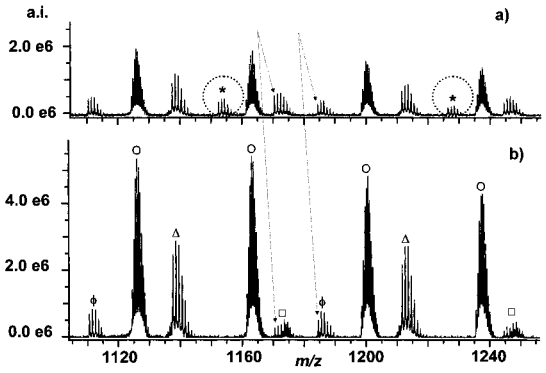

Figure 7. (a) Inset from Figure 6 where NSD was induced. (b) Inset from Figure 1 where relative NSD was not induced.

□ oligomers (Scheme 1). Alternatively, the ϕ distribution could tentatively represent PDMS starting material remnants (i.e., impurities) that were not fully derivatized with two propylamine termini during polymer synthesis. Further evidence in support of this hypothesis is given in the following section.

Nozzle−Skimmer Dissociation. Here, we demonstrate the utility of NSD to determine and verify the identity of polymeric end groups and to determine whether an oligomeric distribution is the result of an energetic fragmentation mechanism. Figure 6 presents a mass spectrum of APS−PDMS measured under NSD-inducing conditions. Parts a and b of Figures 7 illustrate insets from Figures 6 and 1, respectively, over the same *m*/*z* window which by comparison provide information regarding the NSD event. A new oligomeric distribution, evident in Figure 7a, is indicated by *. A proposed mechanism for the nozzle−skimmer fragmentation mechanism is illustrated in Scheme 3. In this mechanism, heterolytic cleavage of a terminal silicon−carbon bond results in the loss of an initially protonated propylamine end group (59 Da) from an intact APS−PDMS oligomer ($\Delta \rightarrow$ *). We believe this mechanism occurs from heterolytic cleavage of a terminal silicon−carbon bond to result in positive charge development on the electropositive silicon. The corresponding zwitterionic fragment which results then decays via intramolecular gas-phase hydrogen transfer from the quaternary nitrogen to the highly nucleophilic carbanion within the propylamine fragment where total charge is conserved to result in a neutral loss. An experimental isotopic pattern of an oligomer from the * distribution is illustrated in Figure 8. The experimental monoisotopic mass of 1152.3610 Da differs from the theoretical monoisotopic mass of the

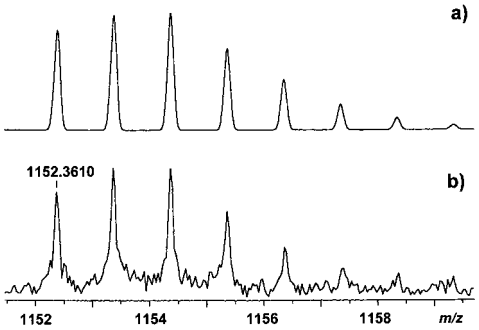

Figure 8. (a) Theoretical and (b) experimental isotopic distribution for $Si_{15}C_{33}N_1H_{98}O_{14}$ from the * distribution.

Scheme 3. Proposed Fragmentation Mechanism for the Neutral Loss of a Propylamine End Group from APS−PDMS Polymer

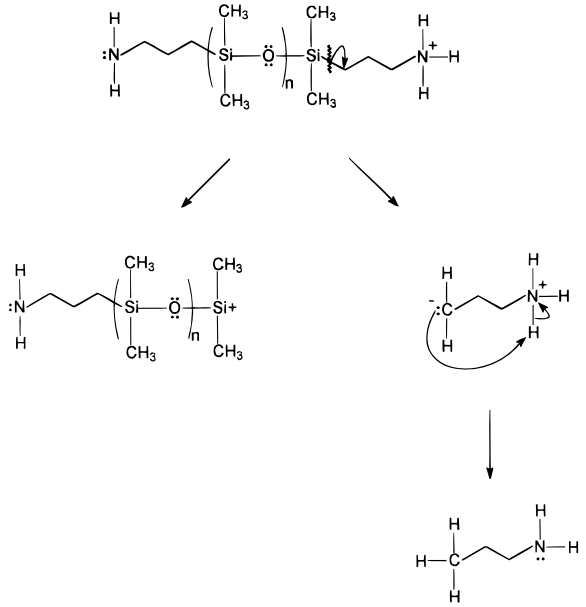

predicted oligomer fragment ($Si_{15}C_{33}N_1H_{98}O_{14}$) by 7.8 ppm, lending validity to this proposed mechanism as the origin of the * profile.

Further, data are readily available to determine whether the □ and ϕ distributions result from energetic fragmentation mechanisms. Specifically, it is expected that the relative ion intensities of oligomer distributions produced by fragmentation will increase because of the greater collisional energy experienced by their precursor ions during the NSD event. Greater collisional energy is obtained by empirically increasing the potential difference between the capillary and skimmer electrodes within the ESI source. Parts a and b of Figure 9 illustrate the change of relative ion intensities for *n*-mers of the □ and ϕ distributions as a function of increasing collisional energy. Figure 9a indicates that the relative ion intensities of *n*-mers from the □ distribution increase as a result of increasing collisional energy. This supports the idea that this distribution is at least in part due to a fragmentation mechanism such as that proposed in Scheme 1. Figure 9b indicates that the relative ion intensities of *n*-mers from the ϕ distribution remain relatively unchanged or decrease with increasing collisional energy. This suggests that this distribution does not occur, to a large extent, from an energetic fragmentation mechanism such as that proposed by Scheme 2. Alternatively, this observation supports the proposal that the ϕ distribution results

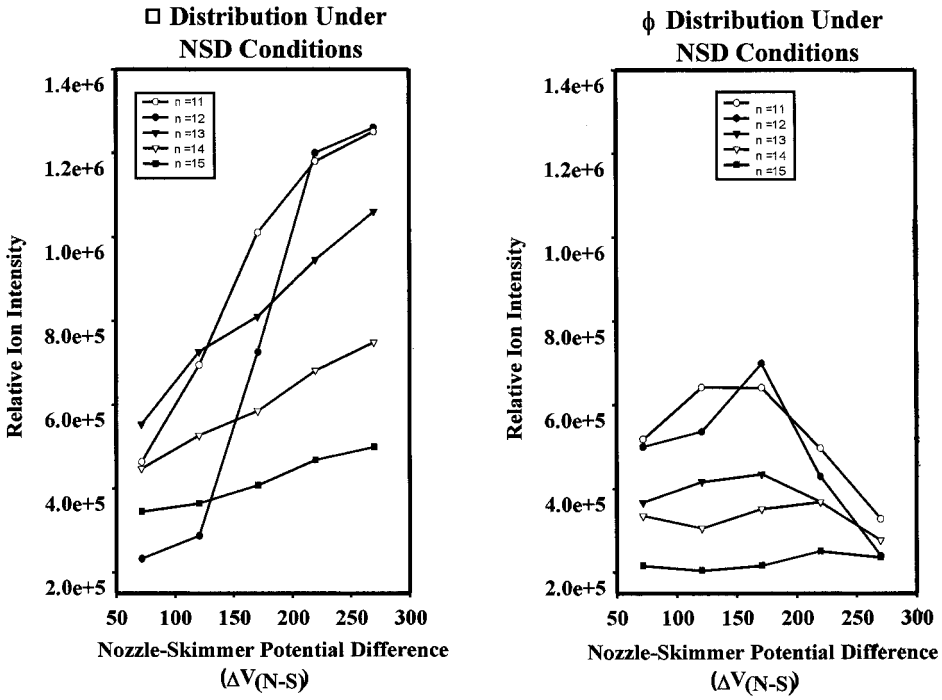

Figure 9. Plot of ion intensities for several oligomers in the (a) □ distribution and (b) ϕ distribution as a function of nozzle−skimmer potential difference. The legend indicating *n*-mer is shown previously.

mainly from PDMS oligomers that were not completely derivatized terminally with propylamine groups and are present as an impurity in the commercial sample. The relative ion intensity shifts for the two oligomeric distributions (□ and ϕ) cannot be a result of mass discrimination because they are observed within the same mass range and under the same experimental conditions. Also, the distributions are not inter-related fragments because a series of such possibilities were evaluated that yielded molecular compositions that are not consistent with the exact masses observed here.

Conclusions

We demonstrate that ESI−FTMS can be used as a valuable analytical technique to accurately determine the elemental composition of polymeric distributions from a hydrophobic synthetic polymer. Accurate mass measurements, enabled by the high RP of FTMS analysis, yielded <10 ppm error for theoretical masses for all polymeric distributions. This attribute coupled with experimental and theoretical isotopic pattern comparisons afforded elemental composition determinations that were used to predict polymer structure including the identification of end groups. The potentials applied to the capillary and skimmer within the ESI source can further be modulated to induce varying degrees of dissociation (NSD) within analyte molecules. Such an experiment was used to determine the identity of the propylamine end groups from a commercial PDMS sample. In addition, NSD was used to qualitatively ascertain the characteristics of two oligomeric distributions known from structural identification not to consist of intact propylamine-terminated PDMS polymer. These results indicate that one distribution occurs predominantly from a fragmentation pathway as validated by the large increase in relative ion abundance as a function of increasing collisional energy during induced NSD.

We propose that the ϕ distribution occurs predominantly as a contaminant in solution as opposed to being a product of fragmentation. The evidence to support this proposal derives from two experimental observations. (1) Under comparatively soft ionization conditions the ϕ distribution was observed. This is striking because the formation of the ϕ distribution from a fragmentation pathway is more energetically disfavored compared to the formation of the □ distribution from an analogous fragmentation pathway. (2) Increasing collisional energy within the ESI source resulted in relatively unchanged or decreased relative ion intensities for n-mers of the ϕ distribution. This result would be expected if a distribution is not a product of a fragmentation mechanism and is in stark contrast to the increasing abundance of the □ and * distributions (fragment ions) with increasing capillary−skimmer dissociation potential difference.

Acknowledgment. We thank Todd Alonzo, Mike Cieslak, Craig Dufresne, and Sarah Lorenz for helpful suggestions. Acknowledgment is made to the donors of the Petroleum Research Fund (administered by the American Chemical Society), the American Society for Mass Spectrometry (Research Award sponsored by the Exxon Education Foundation), and the State University of New York at Buffalo for support of this research.

References and Notes

(1) Schulten, H. R.; Lattimer, R. P. *Mass Spectrom. Rev.* **1984**, *3*, 231−315.
(2) Cook, K. D. In *Encyclopedia of Polymer Science Engineering*; Kroschwitz, J. I., Ed.; Wiley: New York, 1987; Vol. 9, pp 319−56.
(3) Campana, J. E.; Sheng, L.-S.; Shew, S. L.; Winger, B. E. *Trends Anal. Chem.* **1994**, *13*, 239−247.
(4) Smith, C. G.; Smith, P. B.; Pastor, A. J., Jr.; McKelvy, M. L.; Meunier, D. M.; Froelicher, S. W. *Anal. Chem.* **1995**, *67*, 97−126.
(5) Ganesh, K.; Kishore, K. *J. Sci. Ind. Res.* **1995**, *54*, 383−388.
(6) Scrivens, J. H. *Adv. Mass Spectrom.* **1995**, *13*, 447−464.
(7) Wilkins, C. L.; Pastor, S. *Polym. Prepr.* (*Am. Chem. Soc., Div. Polym. Chem.*) **1996**, *37*, 284−285.
(8) Montaudo, G. *Trends Polym. Sci.* **1996**, *4*, 81−86.

(9) Jackson, C. A.; Simonsick, W. J., Jr. *Curr. Opin. Solid State Mater. Sci.* **1997**, *2*, 661−667.
(10) Saf, R.; Mirtl, C.; Hummel, K. *Acta Polym.* **1997**, *48*, 513−526.
(11) Raeder, H. J.; Schrepp, W. *Acta Polym.* **1998**, *49*, 272−293.
(12) Sperling, L. H. *Introduction to Physical Polymer Science*; Wiley-Interscience: New York, 1986.
(13) Kumar, A.; Gupta, R. K. *Fundamentals of Polymers*; McGraw-Hill: New York, 1998.
(14) Matsuo, T.; Matsuda, H.; Katakuse, I. *Anal. Chem.* **1979**, *51*, 1329−1331.
(15) Lattimer, R. P.; Harmon, D. J.; Hanson, G. E. *Anal. Chem.* **1980**, *52*, 1808−1811.
(16) Loo, J. A.; Wang, B. H.; Wang, F. C.-Y.; McLafferty, F. W. *Macromolecules* **1987**, *20*, 698−702.
(17) Macfarlane, R. D. *Trends Anal. Chem.* **1988**, *7*, 179−183.
(18) Lattimer, R. P. *Int. J. Mass Spectrom. Ion Processes* **1984**, *55*, 221; **1992**, *116*, 23−26.
(19) Montaudo, G.; Scamporrino, E.; Puglisi, C.; Vitalini, D. *Macromolecules* **1988**, *21*, 1594−1598.
(20) Vincenti, M.; Pelizzetti, E.; Guarini, A.; Costanzi, S. *Anal. Chem.* **1992**, *64*, 1879−1884.
(21) Benninghoven, A.; Sichtermann, W. K. *Anal. Chem.* **1978**, *50*, 1180−1184.
(22) Bletsos, I. V.; Hercules, D. M.; van Leyen, D.; Hagenhoff, B.; Niehuis, E.; Benninghoven, A. *Anal. Chem.* **1991**, *63*, 1953−1960.
(23) Benninghoven, A. *Angew. Chem., Int. Ed. Engl.* **1994**, *33*, 1023−1043.
(24) Karas, M.; Hillenkamp, F. *Anal. Chem.* **1988**, *60*, 2299−2301.
(25) Tanaka, K.; Waki, H.; Ido, Y.; Akita, S.; Yoshida, Y.; Yoshida, T. *Rapid Commun. Mass Spectrom.* **1988**, *2*, 151−153.
(26) Beavis, R.; Chait, B. *Anal. Chem.* **1990**, *62*, 1836−1840.
(27) Hogan, J. D.; Laude, D. A. *Anal. Chem.* **1992**, *64*, 763−769.
(28) Cotter, R. J.; Honovich, J. P.; Olthoff, J. K.; Lattimer, R. P. *Macromolecules* **1986**, *19*, 2996−3001.
(29) Dole, M.; Mack, L. L.; Rines, R. L.; Mobley, R. C.; Ferguson, L. D.; Alice, M. B. *J. Chem. Phys.* **1968**, *49*, 2240−2249.
(30) Mack, L. L.; Kralik, P.; Rheude, A.; Dole, M. *J. Chem. Phys.* **1970**, *52*, 4977−4986.
(31) Yamashita, M.; Fenn, J. B. *J. Phys. Chem.* **1984**, *88*, 4451−4459.
(32) Whitehouse, C. M.; Dreyer, R. N.; Yamashita, M.; Fenn, J. B. *Anal. Chem.* **1985**, *57*, 675−679.
(33) Fenn, J. B.; Mann, M.; Meng, C. K.; Wong, S. F.; Whitehouse, C. M. *Science* **1989**, *246*, 64−71.
(34) Smith, R. D.; Cheng, X.; Bruce, J. E.; Hofstadler, S. A.; Anderson, G. A. *Nature* **1994**, *369*, 137−139.
(35) O'Connor, P. B.; McLafferty, F. W. *J. Am. Chem. Soc.* **1995**, *117*, 12826− 12831.
(36) Nielen, M. W. F. *Rapid Commun. Mass Spectrom.* **1996**, *10*, 1652−1660.
(37) Latourte, L.; Blais, J. C.; Tabet, J. C.; Cole, R. D. *Anal. Chem.* **1997**, *69*, 2742−2750.
(38) Hunt, S. M.; Sheil, M. M.; Belov, M.; Derrick, P. J. *Anal. Chem.* **1998**, *70*, 1812−1822.
(39) Comisarow, M. B.; Marshall, A. G. *Chem. Phys. Lett.* **1974**, *25*, 282−283.
(40) Marshall, A. G.; Grosshans, P. B. *Anal. Chem.* **1991**, *63*, 215A−229A.
(41) Amster, I. J. *J. Mass Spectrom.* **1996**, *31*, 1325−1337.
(42) Marshall, A. G. *Acc. Chem. Res.* **1996**, *29*, 307−316.
(43) Tolic, L. P.; Anderson, G. A.; Smith, R. D.; Brothers, H. M.; Spindler, R.; Tomalia, D. A. *Int. J. Mass Spectrom. Ion Processes* **1997**, *165*, 405−418.
(44) Hunt, S. M.; Binns, M. R.; Sheil, M. M. *J. Appl. Polym. Sci.* **1995**, *56*, 1589−1597.
(45) Prokai, L.; Simonsick, W. J., Jr. *Rapid Commun. Mass Spectrom.* **1993**, *7*, 853−856.
(46) McEwen, C. N.; Simonsick, W. J., Jr.; Larsen, B. S.; Ute, K.; Hatada, K. J. *J. Am. Soc. Mass Spectrom.* **1995**, *6*, 906−911.
(47) Miola, C.; Delolme, F.; Zanella-Cleon, I.; Dessalces, G.; Hamaide, T. *Polym. Bull.* **1998**, *40*, 541−548.
(48) Festag, R.; Alexandratos, S. D.; Joy, D. C.; Wunderlich, B.; Annis, B.; Cook, K. D. *J. Am. Soc. Mass Spectrom.* **1998**, *9*, 299−304.
(49) Mahon, A.; Kemp, T. J.; Buzy, A.; Jennings, K. R. *Polymer* **1996**, *37*, 531−535.
(50) Padley, H. R.; Bashir, S.; Wood, T. D. *Anal. Chem.* **1997**, *69*, 2914−2918.
(51) Caravatti, P.; Allemann, M. *Org. Mass Spectrom.* **1991**, *26*, 514−518.
(52) Caravatti, P. U.S. Patent 4,924,089.
(53) Dey, M. D.; Castoro, J. A.; Wilkins, C. L. *Anal. Chem.* **1995**, *67*, 1575−1579.
(54) Fei, X.; Murray, K. K. *Anal. Chem.* **1996**, *68*, 3555−3560.
(55) Aaserud, D. J.; Simonsick, W. J., Jr. *Prog. Org. Coat.* **1998**, *34*, 206−213.
(56) Dong, X.; Proctor, A.; Hercules, D. M. *Macromolecules* **1997**, *30*, 63−70.
(57) Dong, X.; Gusev, A.; Hercules, D. M. *J. Am. Soc. Mass Spectrom.* **1998**, *9*, 292−298.
(58) Gardella, J. A., Jr.; Hercules, D. M. *Fresenius' Z. Anal. Chem.* **1981**, *308*, 297−303.
(59) *CRC Handbook of Chemistry and Physics*, 76th ed.; CRC Press: Boca Raton, FL, 1995−1996.

MA981877+